

**MINERALOGY OF THE NIEDERSCHLEMA–ALBERODA U – Se – POLYMETALLIC
DEPOSIT, ERZGEBIRGE, GERMANY. III. FIRST INDICATION
OF COMPLETE MISCIBILITY BETWEEN TENNANTITE AND GIRAUDITE**

HANS-JÜRGEN FÖRSTER[§]

Institute of Earth Sciences, University of Potsdam, P.O. Box 601553, D-14415 Potsdam, Germany

DIETER RHEDE

GeoForschungsZentrum Potsdam, Telegrafenberg, D-14473 Potsdam, Germany

ABSTRACT

Giraudite and hakite, and their more widespread S-dominant analogues, tennantite and tetrahedrite, are locally abundant, but overall rare species in the Niederschlema–Alberoda uranium deposit in the Erzgebirge of Germany. The continuous mercurian giraudite–hakite series, giraudite–tennantite solid solutions, and Se-rich zincian and ferroan tennantite and zincian tetrahedrite are part of the Jurassic selenide mineralization. Extensive, polished-section-scale compositional variation is observed for the giraudite–tennantite series, expressed by the following structural formula (calculated on the basis of 29 atoms per formula unit): $(\text{Cu}_{9.86-10.00}\text{Ag}_{0.00-0.14})_{\Sigma 10} (\text{Cu}^{2+}_{0.18-1.88}\text{Fe}_{0.09-1.77}\text{Zn}_{0.00-1.26}\text{Hg}_{0.00-0.10}\text{Cd}_{0.00-0.06})_{\Sigma 1.95-2.16} (\text{As}_{2.23-4.05}\text{Sb}_{0.00-1.68}\text{Te}_{0.00-0.14}\text{Bi}_{0.00-0.01})_{\Sigma 3.85-4.07} (\text{Se}_{0.00-12.64}\text{S}_{0.32-12.97})_{\Sigma 12.90-13.09}$ ($n = 58$). The solid solutions span the range $\text{gir}_0\text{tn}_{100}$ to $\text{gir}_{98}\text{tn}_2$ with only two minor gaps, suggesting extensive, likely complete miscibility between giraudite and tennantite in nature. Giraudite may contain Hg, Cu, Zn, and Fe as the predominant divalent cation. Cretaceous tennantite, deposited together with Bi–Co–Ni–Ag minerals, is Se-deficient, contains minor amounts of Co and Ni, is enriched in Ag, and may contain appreciable amounts of Bi. Bismuthoan zincian tennantite, the replacement product of wittichenite, contains up to 12.6 wt% Bi (equivalent to 0.97 *apfu*). The origin of the various tennantite–tetrahedrite mineral associations is discussed in the light of the temporal sequence and the activities of selenium and sulfur that prevailed during their formation. The Se-rich and Se-bearing sulfosalts of Jurassic age are suggested to be late-stage species, deposited from low-temperature hydrothermal fluids having an activity of selenium several orders of magnitude lower than that approached during the crystallization of umangite and klockmannite, which mark the peak in $f(\text{Se}_2)$ reached at Niederschlema–Alberoda.

Keywords: giraudite, hakite, tennantite, tetrahedrite, solid solution, miscibility, bismuthoan tennantite, mercury, uranium deposit, Niederschlema–Alberoda, Erzgebirge, Germany.

SOMMAIRE

La giraudite et la hakite, ainsi que leurs analogues à dominance de soufre plus répandus, la tennantite et la tétraédrite, sont localement abondants, mais de façon générale, ce sont des espèces rares au gisement d'uranium de Niederschlema–Alberoda, dans la région de l'Erzgebirge, en Allemagne. Les solutions solides continues entre giraudite et hakite mercuriennes, giraudite et tennantite, et entre tennantite riche en Se zincifère et ferreuse et la tétraédrite zincifère font partie de la minéralisation sélénifère jurassique. Une grande variabilité en composition à l'échelle d'une section polie est observée dans le cas de la série giraudite–tennantite, comme l'exprime la formule structurale suivante, calculée sur une base de 29 atomes par unité formulaire: $(\text{Cu}_{9.86-10.00}\text{Ag}_{0.00-0.14})_{\Sigma 10} (\text{Cu}^{2+}_{0.18-1.88}\text{Fe}_{0.09-1.77}\text{Zn}_{0.00-1.26}\text{Hg}_{0.00-0.10}\text{Cd}_{0.00-0.06})_{\Sigma 1.95-2.16} (\text{As}_{2.23-4.05}\text{Sb}_{0.00-1.68}\text{Te}_{0.00-0.14}\text{Bi}_{0.00-0.01})_{\Sigma 3.85-4.07} (\text{Se}_{0.00-12.64}\text{S}_{0.32-12.97})_{\Sigma 12.90-13.09}$ ($n = 58$). Les solutions solides vont de $\text{gir}_0\text{tn}_{100}$ à $\text{gir}_{98}\text{tn}_2$ avec seulement deux lacunes mineures, ce qui nous mène à proposer une miscibilité complète entre giraudite et tennantite dans la nature. La giraudite peut contenir soit Hg, Cu, Zn, ou Fe comme cation bivalent prédominant. La tennantite crétacée, déposée avec les minéraux de Bi–Co–Ni–Ag, accuse un déficit en Se, contient de quantités mineures de Co et de Ni, est enrichie en Ag, et pourrait contenir des quantités importantes de Bi. La tennantite bismuthifère et zincifère, produit de remplacement de la wittichenite, contient jusqu'à 12.6% de Bi (en poids, l'équivalent de 0.97 atomes par unité formulaire). Nous évaluons l'origine des associations variées des associations de tennantite et de tétraédrite en fonction de la séquence temporelle et de l'activité du sélénium et du soufre au cours de leur formation. Les sulfosels jurassiques porteurs de Se, voire riches en Se, seraient des espèces tardives, déposées à faible température

[§] E-mail address: forhj@gfz-potsdam.de

à partir de fluides hydrothermaux ayant une activité en sélénium plusieurs ordres de grandeur plus faible que celle qui a caractérisé la cristallisation de l'umangite et de la klockmannite, phases qui ont marqué le maximum en $f(\text{Se}_2)$ atteint à Niederschlema-Alberoda.

(Traduit par la Rédaction)

Mots-clés: giraudite, hakite, tennantite, tétraédrite, solution solide, miscibilité, tennantite bismuthifère, mercure, gisement d'uranium, Niederschlema-Alberoda, Erzgebirge, Allemagne.

INTRODUCTION

The unconformity-related, vein-type uranium deposit at Niederschlema-Alberoda in the western Erzgebirge of Germany hosts a complex mineral assemblage comprising uranium minerals, selenides (Förster & Tischendorf 2001, Förster *et al.* 2002, 2003, 2005), sulfides (Förster 2004b), arsenides (Förster *et al.* 2004), tellurides (Förster 2004a), and native elements, which were deposited between the Permian and the Cretaceous. The geology and formation of the Niederschlema-Alberoda deposit have been described in detail by Förster *et al.* (2002, 2003, 2004) and other authors (*e.g.*, Schuppan *et al.* 1994, Lipp 2003). Mining activities focused on selenium between 1961 and 1965 and resulted in a total production of 1472 tonnes of selenium ore containing on average 0.52 wt% Se.

This is part three of a series of papers presenting new results on the mineralogy and origin of this important example of mineralization and concerns the tetrahedrite-tennantite series of minerals. Solid solutions of tennantite and tetrahedrite and their rare Se-dominant analogues, giraudite and hakite, are locally important constituents of the Jurassic and Cretaceous ore assemblages. The Niederschlema-Alberoda deposit was the first in which the existence of a continuous solid-solution series between the mercurian varieties of giraudite and hakite was demonstrated (Förster *et al.* 2002). In this paper, we provide the first evidence for extended, probably complete miscibility between tennantite and giraudite deposited during the main stage of selenide mineralization in Jurassic time. We also report new paragenetic and compositional data on mercurian giraudite-hakite solid solutions and discuss the formation of bismuthoan tennantite during deposition and replacement of Bi-Co-Ni-Fe-As-S minerals during the early Cretaceous.

BACKGROUND INFORMATION

The generalized formula of a half unit-cell of the S-bearing sulfosalts tennantite and tetrahedrite and their rare Se-bearing analogues, giraudite and hakite, can be written $M^+_{10} M^{2+}_2 X^{3+}_4 Y^{2-}_{13}$, where M^+ represents Cu or Ag, M^{2+} represents Cu, Hg, Fe, Zn, Pb, Mn, Co, Ni, and Cd, X stands for As, Sb, Bi, and Te, and Y stands for S and Se.

The Niederschlema-Alberoda deposit hosts the second occurrence of giraudite (ideally $\text{Cu}_{10}\text{Cu}_2\text{As}_4\text{Se}_{13}$)

and one of the five occurrences of hakite (ideally $\text{Cu}_{10}\text{Cu}_2\text{Sb}_4\text{Se}_{13}$) (*e.g.*, Förster *et al.* 2002). The type locality for giraudite is the U-mineralized zone at Chaméane, France; zincian giraudite has the average composition $(\text{Cu}_{9.41}\text{Ag}_{0.59})_{\Sigma 10} (\text{Zn}_{1.09}\text{Cu}^{2+}_{0.82}\text{Hg}_{0.06}\text{Fe}_{0.04})_{\Sigma 2.01} (\text{As}_{2.32}\text{Sb}_{1.63})_{\Sigma 3.95} (\text{Se}_{10.89}\text{S}_{2.15})_{\Sigma 13.04}$ (cations normalized to 29 atoms per formula unit, *apfu*) (Johan *et al.* 1982). The type locality for hakite is Předbořice, Czech Republic; mercurian hakite has an average composition of $\text{Cu}_{10} (\text{Hg}_{1.85}\text{Cu}^{2+}_{0.35})_{\Sigma 2.20} (\text{Sb}_{3.52}\text{As}_{0.63})_{\Sigma 4.15} (\text{Se}_{11.36}\text{S}_{1.31})_{\Sigma 12.67}$ (Johan & Kvaček 1971; see also Brodin *et al.* 1981, Spiridonov *et al.* 1986). In addition to Předbořice, mercurian hakite occurs at Bukov (Johan *et al.* 1978) and Petrovice (Johan 1989), both in the Czech Republic, and at Tuminico, Argentina (Paar *et al.* 2002a, b).

Compositional variability of mercurian giraudite-hakite solid solutions from Niederschlema-Alberoda is expressed by the formula $(\text{Cu}_{9.92-9.99}\text{Ag}_{0.01-0.08})_{\Sigma 10.00} (\text{Hg}_{0.92-1.81}\text{Cu}^{2+}_{0.06-1.12}\text{Zn}_{0.05-0.10}\text{Fe}_{0.00-0.15})_{\Sigma 1.98-2.06} (\text{As}_{0.69-3.98}\text{Sb}_{0.02-3.29})_{\Sigma 3.9-4.08} (\text{Se}_{10.47-11.53}\text{S}_{1.47-2.61})_{\Sigma 12.90-13.09}$ (Förster *et al.* 2002). The solid solutions span the range from $\text{gir}_{99.5}\text{hak}_{0.5}$ to $\text{gir}_{16.2}\text{hak}_{83.8}$, implying complete miscibility between the two selenides for solid solutions containing mercury as the predominant divalent cation.

The sample containing the tennantite-giraudite and mercurian giraudite-hakite solid solutions (HS106) was collected from the dike "Ruhmvoll", at the -510-m level, gallery 414, cross cut 804. Sample S55 is from the dike complex "Saar II", collected at the -810-m level, gallery 23, near the main shaft (No. 371) located in the vicinity of the town of Hartenstein. Sample FS1 was taken from the dike "Bad Elster", at the -390-m level, gallery 28. The location in the Niederschlema-Alberoda ore deposit of the other samples mentioned in this paper is not exactly known.

ANALYTICAL PROCEDURE

The ore minerals were analyzed routinely for Ag, Hg, Cu, Fe, Co, Ni, Zn, Cd, Pb, Pd, Pt, Sb, As, Bi, Te, S, and Se at the GeoForschungsZentrum Potsdam, using an automated Cameca CAMEBAX SX-50 electron microprobe operated in wavelength-dispersion mode. The operating conditions were as follows: accelerating voltage 20 kV, beam current 40 nA, and beam diameter 1–2 μm . The counting times on the peak chosen were between 30 and 80 s, and half that time for background

counts on each side of the peak. Data reduction was done with a PAP correction procedure (Pouchou & Pichoir 1985).

X-ray spectral lines measured in Bi-free minerals were $K\alpha$ for Fe, Co, Ni, Cu, Zn, Se, and S, $K\beta$ for As, $L\alpha$ for Hg, Pd, Pt, Cd, Sb, and Te, $L\beta$ for Ag, $M\alpha$ for Bi, and $M\beta$ for Pb. Peak interferences in Bi-bearing tennantite were avoided by selecting different spectra for As, Ag (both $L\alpha$), and Pb ($M\alpha$). Primary standards included pure metals for Co, Pd, and Pt, chalcopyrite for Fe, Cu, and S, pentlandite for Ni, sphalerite for Zn, cinnabar for Hg, Ag_2Te for Ag and Te, galena for Pb, GaAs for As, Bi_2Se_3 for Bi and Se, InSb for Sb, and CdS for Cd. Typical detection-limits for the individual elements were between 0.04 and 0.07 wt%.

RESULTS

Petrographic description and mineral assemblages

Tetrahedrite–tennantite solid solutions are part of various ore-mineral assemblages, which relate to different mineralizing events that produced the complex deposit at Niederschlema–Alberoda. Tennantite–giraudite solid solutions occur, together with hakite–giraudite solid solutions, in sample HS 106. The complex min-

eral associations in this sample also include tiemannite (HgSe), clausthalite (PbSe), eucairite (CuAgSe), eskebornite (CuFeSe₂), hessite (Ag₂Te), native Te, berzelianite (Cu_{2-x}Se), umangite (Cu₃Se₂), klockmannite (CuSe) – ferroselite (FeSe) solid solutions (?), jolliffeite (NiAsSe), löllingite, chalcopyrite, pyrite, and native As. The sequence of crystallization of the various minerals in this sample is not easy to deduce. The proposed sequence is löllingite ⇒ berzelianite ⇒ umangite ⇒ klockmannite–ferroselite s.s. ⇒ hessite ⇒ native Te ⇒ clausthalite ⇒ jolliffeite ⇒ eskebornite ⇒ tiemannite ⇒ mercurian hakite–giraudite s.s. ⇒ zincian or ferroan giraudite ⇒ giraudite–tennantite s.s. ⇒ chalcopyrite ⇒ pyrite ⇒ native As.

The tennantite–giraudite solid solutions form grains of different size, shape, and pattern of zonation. The anhedral grain shown in Figure 1, which displays the extent of miscibility between tennantite and giraudite most completely (see next section), shows a complex growth-pattern involving patchy zonation and bright, band-like zones at or close to the rim of the grain. Sulfurian eskebornite occurs inside and overgrows the grain. A narrow, dark band in the least bright part of the grain indicates that the final growth of the grain was interrupted by the precipitation of chalcopyrite. The sulfurian eskebornite, with its characteristically mottled

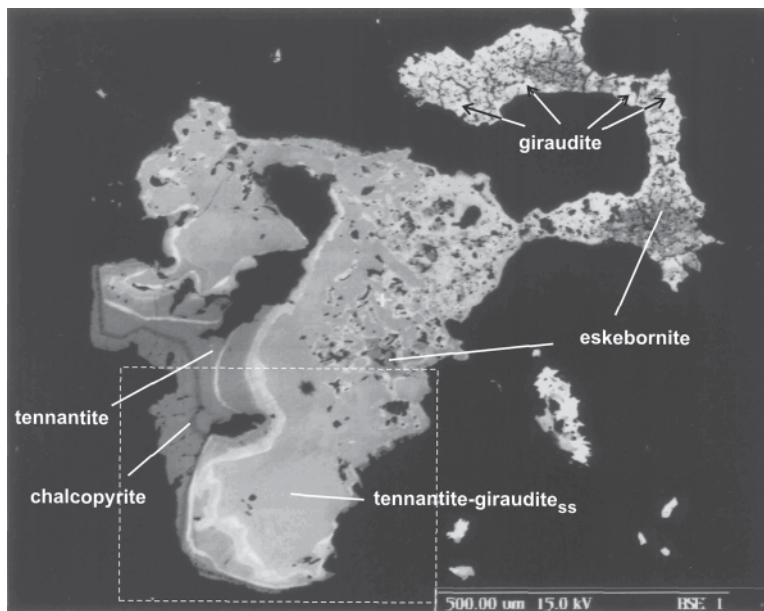


FIG. 1. Back-scattered electron (BSE) image of a polymineralic aggregate in sample HS106 composed of a cuprian and zincian tennantite–giraudite solid solution, cuprian and ferroan giraudite, ferroan tennantite, sulfurian eskebornite, and chalcopyrite. The different brightness in the eskebornite grain in the upper right corner is due to variation in the Se:S ratio. Scale bar: 0.5 mm.

appearance, contains several small grains of giraudite. The textural relations suggest that the tennantite–giraudite replaced the eskebornite.

The tennantite–giraudite grain in Figure 2 is euhedral to subhedral, displays mainly a systematic, fine pattern of zonation parallel to the crystal rims. This grain postdates and overgrows an aggregate composed of tiemannite and mercurian giraudite. Mercurian giraudite–hakite solid solutions typically occur in intimate association with tiemannite, but also form individual grains in the matrix. Another selenide-bearing ore assemblage, which contains tennantite, consists of clausthalite + chalcopyrite ± naumannite ± löllingite ± uraninite, but lacks giraudite and hakite. Tennantite also is present in a sample (R4) that contains the only grain of tetrahedrite observed during this study. This small (20 µm) grain of tetrahedrite occurs between grains of clausthalite and naumannite. The ore assemblage in sample R4 is complex and in addition includes eucairite, umangite, eskebornite, bukovite (Cu₃FeTl₂Se₄), and late löllingite–rammelsbergite solid solutions.

Anhedral grains of Bi-bearing tennantite, with a size between a few µm and more about 400 µm, are dispersed in the ankerite–siderite matrix or form intergrowths with other sulfides and arsenides. The highest Bi contents are observed in grains overgrowing and replacing wittichenite. Associated minerals include chalcopyrite, chalcocite, bornite, gersdorffite, and löllingite–safflorite solid solutions. Tennantite also forms part of an assemblage rich in sulfides but poor in arsenides. This tennantite is included in chalcocite and associated with bornite, pyrite, chalcopyrite, and minor rammelsbergite.

Chemical composition

Representative results of electron-microprobe analyses of the various tetrahedrite–tennantite minerals formed at Niederschlema–Alberoda are given in Tables 1–5. X-ray element-distribution maps for a tennantite–giraudite solid solution and a mineral aggregate including zoned selenite tennantite, mercurian hakite, and mercurian giraudite, are shown in the Figures 2 and 3b–f, respectively.

Tennantite–giraudite solid solutions in sample HS106 show a wide range of compositions (Table 1). Copper predominates at the *M*⁺ site, accompanied by minor amounts of Ag (<0.3 wt%). Copper, iron, or zinc are the dominant divalent species. Mercury (<1 wt%) and Cd (<0.4 wt%) are minor substituents at the *M*²⁺ site. The most Se-poor members of the series tend to be rich in Fe (Table 1, anal. 1–3), whereas copper occupies most of the *M*²⁺ site in the most Se-rich giraudite (Table 1, anal. 14–15). Zinc is predominant in parts of the bright Se-rich band in the grain shown in Figure 1, which contains appreciable amounts of Sb substituting for As (Table 1, anal. 8; Figs. 2a, d, f). In all other tennantite–giraudite solid solutions, Sb occupies less

than 5 mole % of the *X*³⁺ site. Tellurium is present usually at concentrations <0.1 wt%, with the exception of the composition closest to end-member cuprian giraudite, which contains 0.6 wt% Te (Table 1, anal. 15). The measured compositions span the range between the two end-members tennantite and giraudite with only two minor gaps, between about 6.3 and 8.0 and between 9.1 and 10.5 *apfu* Se (Table 1, Fig. 4). Most of this variation is recorded in the single grain shown in Figures 1 and 2. The range in composition of the tennantite–giraudite solid solutions in sample HS106 is expressed by (Cu_{9.86–10.00}Ag_{0.00–0.14})Σ₁₀ (Cu²⁺_{0.18–1.88}Fe_{0.09–1.77}Zn_{0.00–1.26}Hg_{0.00–0.10}Cd_{0.00–0.06})Σ_{1.95–2.16} (As_{2.23–4.05}Sb_{0.00–1.68}Te_{0.00–0.14}Bi_{0.00–0.01})Σ_{3.85–4.07} (Se_{0.00–12.64}S_{0.32–12.97})Σ_{12.90–13.09} (*n* = 58).

Copper is the dominant element among the monovalent species in mercurian hakite–giraudite solid solutions from sample HS106 (Table 2). Silver is present at a maximum of 1.3 wt%, which is equivalent to 0.29 *apfu*. Mercury is the most prominent divalent element, with concentrations between 13.7 and 16.9 wt%, equivalent to 1.65–1.99 *apfu* (Fig. 5a). Iron accounts for 0–0.31 *apfu*, and Cu* [calculated as Cu_{tot} – (10 – Ag_{tot})], for 0–0.22 *apfu*. The concentrations of As and Sb range considerably, As from 2 to 13.3 wt% (0.64–4.02 *apfu*), and Sb from 0 to 15.9 wt% (0–3.31 *apfu*) (Fig. 5b). The solid solutions are poor in S substituting for Se. Mercurian hakite contains between 0.55 and 1.25 wt% S (0.41–0.94 *apfu*; Fig. 5c), and mercurian giraudite, between 0.15 and 2.3 wt% (0.11–1.63 *apfu*). Compositional heterogeneity is expressed in the results of 28 point-analyses: (Cu_{9.64–10.00}Ag_{0.00–0.29})Σ_{9.85–10} (Hg_{1.65–1.99}Fe_{0.00–0.31}Cu_{0.00–0.22}Cd_{0.00–0.02})Σ_{1.95–2.16} (As_{0.65–4.02}Sb_{0.00–3.35}Bi_{0.00–0.01})Σ_{3.87–4.13} (Se_{11.32–12.82}S_{0.11–1.63})Σ_{12.89–13.14}.

Tennantite associated with clausthalite + löllingite ± naumannite ± chalcopyrite ± uraninite is either a zincian, ferroan, or cuprian variety (Table 3). Tennantite from this particular assemblage usually is poor in Ag (<1.7 wt%), Hg (<0.3 wt%) and Bi (<0.2 wt%), variable with respect to Sb (0.0–5.8 wt%), and contains Se (1.3–14 wt%) substituting for S. Compositional variation is expressed by the formula (Cu_{9.67–10.00}Ag_{0.00–0.22})Σ_{9.90–10} (Zn_{0.20–1.67}Fe_{0.27–1.37}Cu_{0.00–1.13}Hg_{0.00–0.02}Cd_{0.00–0.01})Σ_{1.92–2.06} (As_{3.31–4.02}Sb_{0.04–0.73}Te_{0.00–0.01})Σ_{3.86–4.12} (S_{10.32–12.81}Se_{0.25–2.85})Σ_{12.95–13.21} (*n* = 46). Tetrahedrite intergrown with PbSe and Ag₂Se is enriched in As (7.2–9 wt%) and Se (4.3–4.9 wt%). The average composition of this Se-rich intermediate member of the zincian tetrahedrite–tennantite series is (Cu_{9.82}Ag_{0.18})Σ₁₀ (Zn_{1.70}Fe_{0.20}Cu_{0.06}Hg_{0.01})Σ_{1.97} (Sb_{2.21}As_{1.77})Σ_{3.98} (S_{12.10}Se_{0.95})Σ_{13.05} (*n* = 2).

Tennantite associated with wittichenite, gersdorffite, and löllingite–safflorite solid solutions is mostly of the zincian variety (Table 4). Silver, Hg, Cd, and Se are minor constituents. Noteworthy are minor contents of Co and Ni, up to 0.55 wt% (0.14 *apfu*) each. The Sb-for-As and Bi-for-As substitutions are extensive. Antimony ranges between 0 and 36 mole %, and Bi, between

TABLE 1. CHEMICAL COMPOSITION OF TENNANTITE–GIRAUDITE SOLID SOLUTIONS FROM SAMPLE HS106

Anal. No	1	2	3	4	5	6	7	8	9	10	11	12	13	14	15
Cu wt%	44.16	44.03	43.99	45.08	44.15	44.03	42.03	40.82	38.04	39.84	36.32	34.05	36.18	37.17	36.49
Ag	d.l.	d.l.	d.l.	d.l.	d.l.	d.l.	0.06	d.l.	0.12	d.l.	d.l.	0.10	0.12	d.l.	0.05
Hg	d.l.	0.04	d.l.	0.33	d.l.	d.l.	0.28	d.l.	0.13	0.10	0.64	0.64	1.03	0.21	0.29
Zn	0.17	d.l.	0.03	0.00	3.15	3.22	3.49	2.30	4.64	2.31	1.79	1.44	1.72	d.l.	d.l.
Cd	d.l.	d.l.	d.l.	0.07	0.05	0.09	0.17	0.12	0.38	0.10	0.09	0.08	0.10	d.l.	d.l.
Fe	6.68	6.68	5.43	3.82	1.04	0.55	0.61	1.43	0.33	1.01	2.07	3.86	1.02	0.70	0.34
As	20.45	19.40	19.64	19.65	19.06	18.63	17.34	16.68	9.44	16.50	15.67	15.72	15.72	15.00	14.38
Sb	d.l.	1.18	d.l.	d.l.	0.30	0.27	1.31	1.39	11.57	1.08	0.14	0.21	0.22	d.l.	d.l.
Bi	d.l.	d.l.	0.06	d.l.	d.l.	d.l.	d.l.	d.l.	d.l.	d.l.	d.l.	0.05	0.09	d.l.	d.l.
Te	d.l.	d.l.	d.l.	d.l.	d.l.	d.l.	d.l.	d.l.	d.l.	0.06	0.10			0.04	0.62
S	28.27	28.08	25.32	23.91	22.91	20.88	18.35	15.80	15.61	13.47	7.73	6.77	6.75	2.44	0.49
Se	d.l.	0.52	5.12	8.22	9.07	12.99	16.61	21.16	19.60	25.34	35.44	37.40	36.57	45.03	48.05
Total	99.73	99.94	99.59	101.07	99.73	100.66	100.25	99.70	99.87	99.75	99.88	100.31	99.51	100.59	100.73
Cu <i>apfu</i>	10.00	10.00	10.00	10.00	10.00	10.00	9.99	10.00	9.98	10.00	10.00	9.98	9.98	10.00	9.99
Ag							0.01		0.02			0.02	0.02		0.01
sum <i>M</i> ⁺	10.00	10.00	10.00	10.00	10.00	10.00	10.00	10.00	10.00	10.00	10.00	10.00	10.00	10.00	10.00
Cu*	0.22	0.23	0.53	0.87	0.90	1.04	0.94	0.96	0.62	1.00	0.76	0.18	0.98	1.74	1.88
Hg				0.02			0.02		0.01	0.01	0.06	0.06	0.10	0.02	0.03
Zn	0.04		0.01		0.76	0.79	0.88	0.60	1.26	0.62	0.52	0.42	0.50		
Cd				0.01	0.01	0.01	0.02	0.02	0.06	0.02	0.01	0.01	0.02		
Fe	1.76	1.77	1.48	1.05	0.29	0.16	0.18	0.44	0.11	0.32	0.70	1.31	0.35	0.25	0.13
sum <i>M</i> ²⁺	2.02	2.00	1.92	1.95	2.06	1.99	2.05	2.02	2.06	1.96	2.04	1.98	1.95	2.01	2.03
As	4.01	3.82	3.99	4.02	3.99	3.96	3.83	3.80	2.23	3.86	3.94	3.98	4.04	4.02	3.97
Sb		0.14			0.04	0.04	0.18	0.19	1.68	0.16	0.02	0.03	0.03		
Bi													0.01		
Te										0.01	0.01			0.01	0.10
sum <i>Y</i> ³⁺	4.01	3.96	3.99	4.02	4.03	4.00	4.01	3.99	3.91	4.03	3.97	4.01	4.08	4.03	4.07
S	12.97	12.93	12.01	11.43	11.21	10.38	9.46	8.41	8.63	7.38	4.54	4.00	4.05	1.53	0.32
Se		0.10	0.99	1.59	1.80	2.62	3.48	4.57	4.40	5.63	8.45	8.98	8.92	11.44	12.58
sum <i>Z</i> ²⁻	12.97	13.03	13.00	13.02	13.01	12.98	12.94	12.98	13.03	13.01	13.00	12.98	12.97	12.97	12.90

The number of ions is normalized to 29 atoms per formula unit (*apfu*); blank: not analyzed. d.l.: detection limit. Cu* calculated as $Cu_{tot} - (10 - Ag_{tot})$. Anal. 1–4: ferroan tennantite, 5–8, 10: cuprian tennantite, 9: zincian tennantite, 11, 13, 14–15: cuprian giraudite, 12: ferroan giraudite. Compositions 1–13 are taken from the grain shown in Figure 1.

0 and 24 mole % of the X^{3+} site. No correlation exists between the amounts of divalent and trivalent cations.

Se-poor tennantite from the assemblage chalcocite + bornite + pyrite + chalcopyrite ± rammelsbergite in the two samples from this study (Sh117, Sh126) differs slightly in composition. Cuprian tennantite from sample Sh117 contains between 1.3 and 3.1 wt% Ag substituting for Cu, and 0.2–0.6 wt% Sb and 0.2–3.5 wt% Bi substituting for As (Table 5). Its average formula is $(Cu_{9.74}Ag_{0.26})_{\Sigma 10} (Cu_{1.07}Zn_{0.54}Fe_{0.45}Ni_{0.02})_{\Sigma 2.08} (As_{3.80}Bi_{0.10}Sb_{0.05})_{\Sigma 3.95} (S_{12.95}Se_{0.01})_{\Sigma 12.96}$ ($n = 7$). Ferroan-cuprian tennantite from sample Sh126 contains 2.2–2.9 wt% Ag and has an average composition of $(Cu_{9.65}Ag_{0.35})_{\Sigma 10} (Cu_{0.73}Fe_{0.72}Zn_{0.51}Hg_{0.01})_{\Sigma 1.97} (As_{3.98}Bi_{0.02}Sb_{0.01})_{\Sigma 3.01} (S_{13.90}Se_{0.01})_{\Sigma 13.01}$ ($n = 5$).

DISCUSSION

Miscibility in the tetrahedrite–tennantite series

Complete substitution between the S-dominant end-members tetrahedrite and tennantite is evident for solid solutions with Hg, Zn, or Fe fully occupying the M^{2+} position (*e.g.*, Johnson *et al.* 1986, Foit & Ulbricht 2001). The data from this study provide confirmation of complete substitution between the Se-dominant end-members hakite and giraudite containing Hg as the predominant divalent cation (*e.g.*, Förster *et al.* 2002). We demonstrate that mercury may fully occupy the M^{2+} position in both giraudite and hakite. Our new compositional data also fill the small gap between 2.6 and 3.6

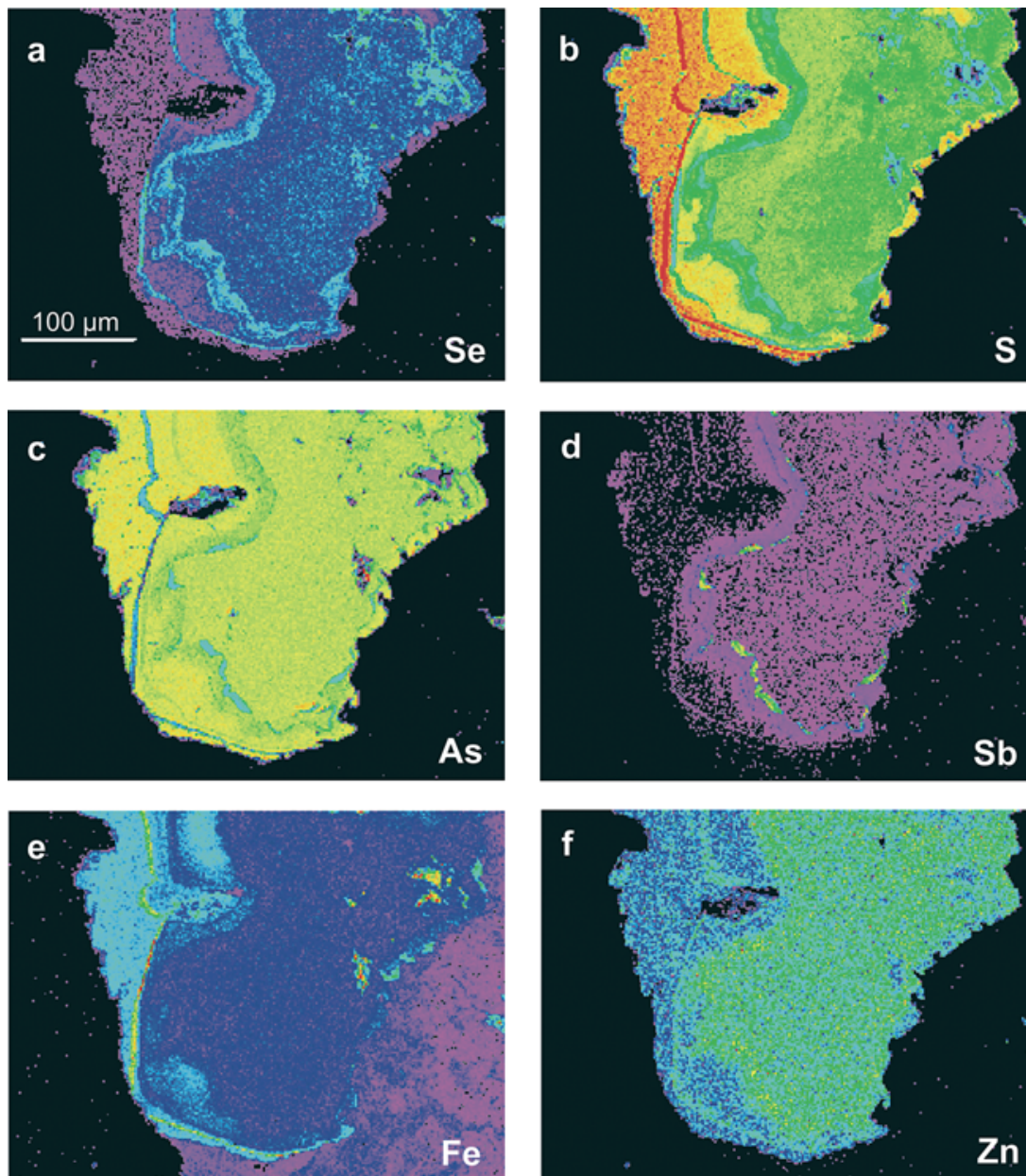


FIG. 2. X-ray element distribution maps for Se (a), S (b), As (c), Sb (d), Fe (e), and Zn (f) in the tennantite-giraudite solid solution shown in Figure 1. The area of the X-ray maps corresponds to the dashed box in Figure 1. The lowest concentrations of an element are shown by cold colors (blue – violet), whereas the highest accumulations are shown in warm colors (red – orange).

apfu As (and correspondingly 0.4–1.4 *apfu* Sb; see Fig. 5c) observed in the first study of mercurian hakite-giraudite solid solutions from Niederschlema-Alberoda (Förster *et al.* 2002, their Fig. 4b). In this study, we provide the first evidence for extensive substitution

FIG. 3. (a) BSE image showing a selenide-sulfide paragenesis in sample HS106 (1: tiemannite, 2: mercurian giraudite, 3: mercurian hakite, 4: ferroan tennantite, 5: umangite), and X-ray element-distribution maps for Hg (b), Se (c), S (d), Sb (e) and As (f). The dashed line in Figure 3b encloses the area covered by Figure 3a.

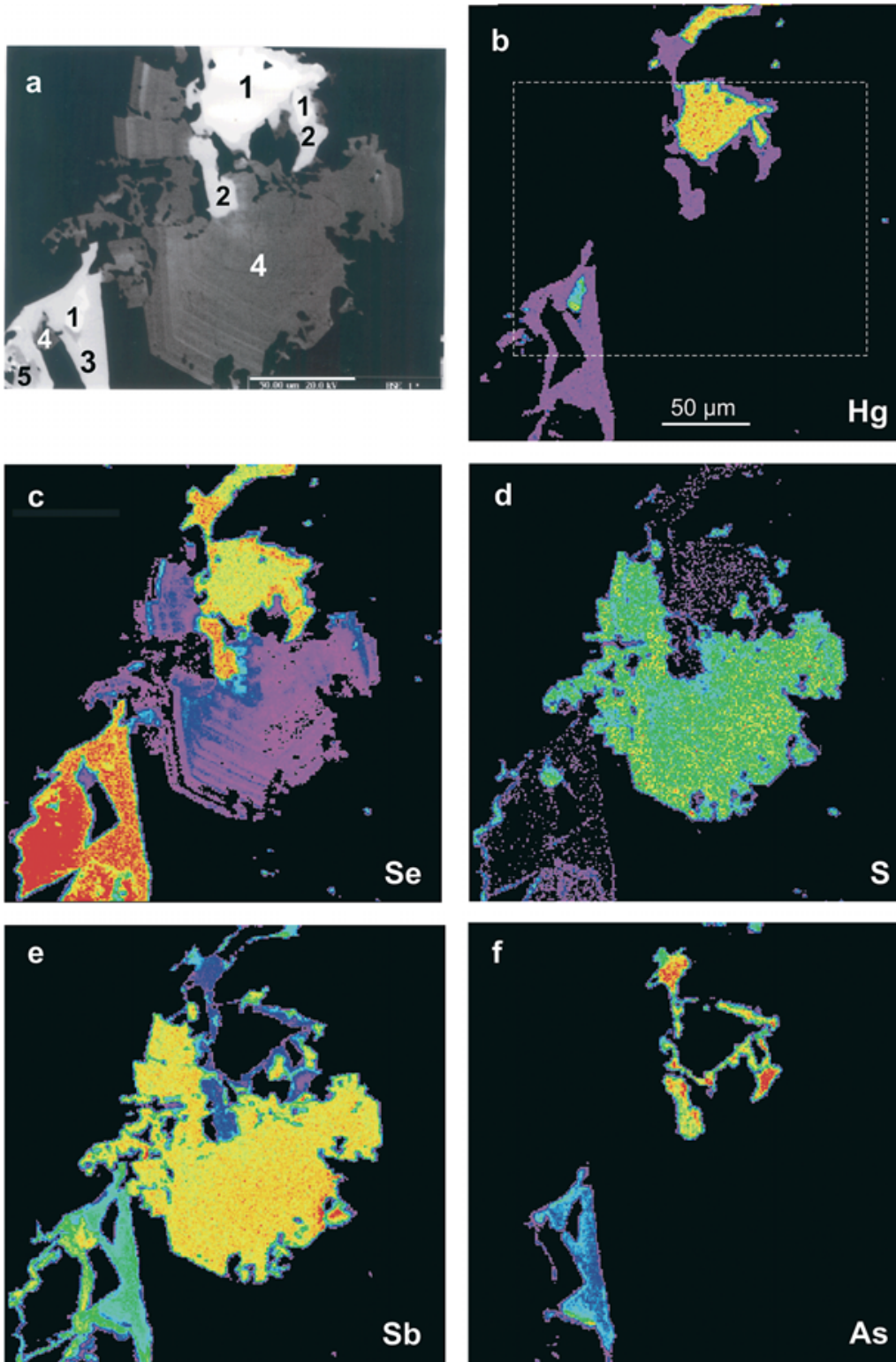


TABLE 2. CHEMICAL COMPOSITION OF MERCURIAN HAKITE–GIRAUDITE SOLID SOLUTIONS FROM SAMPLE HS106

Cu wt%	24.94	25.27	26.54	25.95	26.28	26.47	26.45	27.97
Ag	1.23	1.01	0.78	0.76	0.80	0.75	1.02	d.l.
Hg	16.04	15.51	13.73	16.04	15.56	16.02	16.69	15.72
Cd	d.l.	d.l.	d.l.	0.03	d.l.	0.04	d.l.	d.l.
Fe	0.10	0.34	0.26	0.29	0.26	0.31	0.20	0.77
As	2.21	2.81	4.35	5.98	8.50	10.21	12.80	13.26
Sb	15.88	14.95	12.96	10.62	6.52	4.23	0.03	d.l.
Bi	0.05	d.l.	d.l.	0.04	d.l.	0.04	d.l.	d.l.
Te	d.l.	d.l.	d.l.	d.l.	d.l.	d.l.	d.l.	d.l.
S	0.80	0.66	0.74	1.25	0.68	0.72	0.15	2.31
Se	39.36	40.16	41.08	39.67	41.28	41.50	43.05	39.53
Total	100.67	100.71	100.43	100.62	99.88	100.27	100.40	99.56
Cu <i>apfu</i>	9.71	9.77	9.83	9.79	9.82	9.83	9.78	9.96
Ag	0.29	0.23	0.17	0.17	0.18	0.16	0.22	
sum M^{2+}	10.00	10.00	10.00	9.96	10.06	9.99	10.00	9.96
Cu ⁺	0.02		0.22		0.05		0.01	
Hg	1.98	1.90	1.65	1.92	1.85	1.88	1.96	1.77
Cd				0.01		0.01		
Fe	0.05	0.15	0.11	0.12	0.11	0.13	0.08	0.31
sum M^{2+}	2.05	2.05	1.98	2.05	2.01	2.02	2.05	2.08
As	0.73	0.92	1.39	1.91	2.71	3.22	4.02	4.00
Sb	3.23	3.02	2.56	2.09	1.28	0.82	0.01	
Bi	0.01			0.01				
sum Y^{3+}	3.97	3.94	3.95	4.01	3.99	4.04	4.03	4.00
S	0.62	0.50	0.56	0.94	0.51	0.53	0.11	1.63
Se	12.36	12.50	12.51	12.05	12.49	12.41	12.82	11.32
sum Z^{2-}	12.98	13.00	13.07	12.99	13.00	12.94	12.93	12.95

The number of ions is normalized to 29 atoms per formula unit (*apfu*); blank: not analyzed; d.l.: detection limit. Cu⁺ is calculated as Cu_{tot} - (10 - Ag_{tot}).

between S- and Se-dominant end-members. We relate the two small gaps in the Se *versus* S substitution (see Fig. 5b) to the local environment of formation of the ore assemblage in sample HS106, which certainly did not involve the entire possible Se *versus* S range in the mineral-depositing fluid. We do not suggest that these gaps are a reflection of limited miscibility between the end-members, for which also no crystallochemical reason appears to exist. Our data imply that a continuous miscibility exists between tennantite and giraudite for solid solutions with Cu, Zn, or Fe fully occupying the M^{2+} position. Giraudite may not contain only Zn (Johan *et al.* 1982) and Hg (Förster *et al.* 2002), but also Cu and Fe as the predominant divalent cation (Fig. 6). Available analytical data show that in near-end-member giraudite, either Hg or Cu predominate, whereas Zn, and especially Fe, may predominate at the M^{2+} position in less Se-rich giraudite. This overall variability contrasts with that of its Sb-dominant analogue, hakite, in which Hg invariably predominates at the M^{2+} position.

Compositions intermediate between hakite and tetrahedrite have not yet been observed. The zincian tetrahedrite from Niederschlema–Alberoda (*e.g.*, Table 3, anal. 10), which contains a maximum of 4.85 wt% Se (equivalent to 1.01 *apfu*), is the most Se-rich, Te-poor tetrahedrite reported to date. Prior to this study, a sample of zincian tetrahedrite from the Ozernoe volcanogenic Au–Ag–Te deposit in Kamchatka (Russia), containing 1.2 wt% Se, was reported as the most Se-rich, Te-poor tetrahedrite (*e.g.*, Spiridonov *et al.* 1990). Tellurian tet-

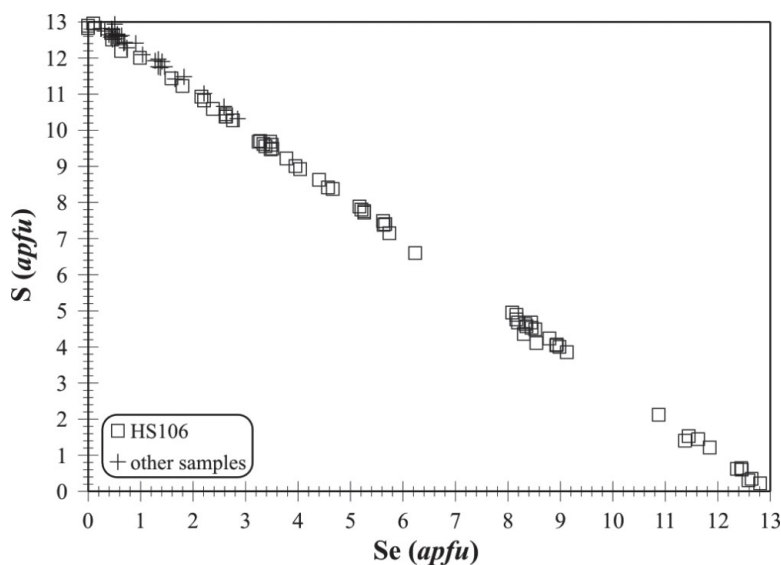


FIG. 4. Plot (in *apfu*) of S *versus* Se for cuprian, zincian and ferroan tennantite–giraudite solid solutions in sample HS106 and other samples (see Tables 1 and 3–5) from Niederschlema–Alberoda.

TABLE 3. CHEMICAL COMPOSITION OF TENNANTITE AND TETRAHEDRITE ASSOCIATED WITH CLAUSTHALITE

sample anal. no.	R4 1	R6 2	R6 3	R6 4	R6 5	R6 6	R6 7	8157 ¹⁾ 8	FS1 9	R4 10	R4 11
Cu wt%	43.45	42.02	41.92	42.07	42.53	42.39	42.03	39.85	44.74	37.94	38.74
Ag	d.l.	d.l.	0.90	0.22	0.10	0.11	d.l.	d.l.	d.l.	2.18	0.20
Hg	0.21	d.l.	0.04	0.14	d.l.	d.l.	0.05	0.17	d.l.	0.16	d.l.
Zn	1.74	3.31	3.16	4.02	3.90	4.59	4.86	6.82	0.84	6.79	6.81
Cd	0.04	d.l.	d.l.	d.l.	d.l.	0.07	d.l.	0.03	d.l.	0.05	d.l.
Fe	4.05	4.48	4.49	3.74	3.62	3.33	3.16	0.94	1.18	0.65	0.72
As	16.31	19.25	18.96	17.83	17.75	18.95	19.06	18.21	19.06	7.17	8.99
Sb	5.14	0.93	1.23	2.96	2.52	1.66	1.16	0.34	d.l.	17.50	15.29
Bi	d.l.	d.l.	d.l.	d.l.	d.l.	d.l.	d.l.	0.05	d.l.	d.l.	d.l.
S	26.70	26.52	26.51	26.83	26.27	27.45	25.99	20.86	22.04	23.38	23.99
Se	1.66	3.70	2.48	2.77	3.55	1.33	3.88	12.96	10.86	4.85	4.34
Total	99.31	100.22	99.69	100.55	100.23	99.89	100.19	100.23	99.72	100.67	99.08
Cu <i>apfu</i>	10.00	9.93	9.87	9.96	9.99	9.98	10.00	10.00	10.00	9.67	9.95
Ag			0.13	0.03	0.01	0.01				0.33	0.03
sum <i>M</i> ⁺	10.00	9.93	10.00	9.96	10.00	9.99	10.00	10.00	10.00	10.00	9.98
Cu*	0.45		0.10		0.14		0.01	0.04	1.13	0.15	
Hg	0.02			0.01				0.01		0.01	
Zn	0.41	0.76	0.73	0.92	0.90	1.05	1.12	1.67	0.20	1.71	1.70
Cd	0.01					0.01				0.01	
Fe	1.11	1.21	1.22	1.01	0.98	0.89	0.86	0.27	0.62	0.19	0.21
sum <i>M</i> ²⁺	2.00	1.97	2.05	1.94	2.02	1.95	1.99	1.99	1.94	2.07	1.91
As	3.33	3.86	3.83	3.58	3.59	3.79	3.85	3.89	4.02	1.57	1.96
Sb	0.64	0.11	0.15	0.37	0.31	0.20	0.14	0.04		2.36	2.05
sum <i>Y</i> ³⁺	3.97	3.97	3.98	3.95	3.90	3.99	3.99	3.93	4.02	3.93	4.01
S	12.73	12.42	12.50	12.59	12.40	12.81	12.27	10.42	10.86	11.99	12.21
Se	0.32	0.70	0.47	0.53	0.68	0.25	0.74	2.63	2.17	1.01	0.90
sum <i>Z</i> ²⁻	13.05	13.12	12.97	13.12	13.08	13.06	13.01	13.05	13.03	13.00	13.11

The number of ions is normalized to 29 atoms per formula unit (*apfu*); d.l.: detection limit. Cu* is calculated as $Cu_{tot} - (10 - Ag_{tot})$. ¹⁾ Taken from Förster & Tischendorf (2001). Anal. 1–5: ferroan tennantite, anal. 6–8: zincian tennantite, anal. 9: cuprian tennantite, anal. 10, 11: zincian tetrahedrite.

rahedrite and goldfieldite may contain up to 2.8 *apfu* Se (e.g., Spiridonov & Okrugin 1985, Trudu & Knittel 1998). Mercurian hakite is reported (Johan & Kvaček 1971, Paar *et al.* 2002b) to contain sulfur in contents less than 2.63 *apfu* (e.g., Fig. 5c). Currently, the gaps in the hakite–tetrahedrite solid-solution series span the range from 1–10 *apfu* Se (for Te-poor tetrahedrite) or 3–10 *apfu* Se (considering Te-rich tetrahedrite), respectively.

Bismuthoan zincian tennantite from Niederschlema–Alberoda, which contains a maximum of 12.6 wt% Bi (equivalent to 0.97 *apfu*), is among the tetrahedrite–tennantite solid solutions richest in Bi (Fig. 7). Tennantite slightly more enriched in Bi has been reported from (a) the Tyrnyauz Mo–W deposit in Russia (13.9 wt% Bi, 1.11 *apfu*; Vinogradova *et al.* 1985), (b) the Jubilejno–Shegirikhinsk pyrite–polymetallic deposit in Russia (16.7 wt% Bi, 1.36 *apfu*; Sergeeva & Shatagin 1980), (c) the Altenberg Sn–W deposit in the eastern Erzgebirge of Germany (17 wt% Bi, 1.36 *apfu*; Förster *et al.* 1986), and (d) the Mangualde pegmatite in Portugal studied by Oen & Kieft (1976), where the

tennantite has incorporated up to 19.15 wt. Bi (1.57 *apfu*). All these examples of bismuthoan tennantite share the common feature of being of the zincian variety.

Formation of the various tetrahedrite–tennantite-bearing ore assemblages

The three selenide-associated solid-solution series, between giraudite and hakite, giraudite and tennantite, and tennantite and tetrahedrite, most probably formed in the Jurassic, when the bulk of the selenides were deposited. From the textural and compositional relations between the sulfosalts and the associated minerals, we infer that the mercurian giraudite–hakite series predates the giraudite–tennantite solid solutions. Taking into consideration that naumannite and clauthalite are among the late-formed Jurassic selenides at Niederschlema–Alberoda, the Se-bearing tennantite and tetrahedrite species (Table 3) should be the youngest of these three solid-solution series.

The first mercurian giraudite–hakite grain from Niederschlema–Alberoda described by Förster *et al.*

TABLE 4. CHEMICAL COMPOSITION OF ZINCIAN TENNANTITE FROM THE Bi-Co-Ni ASSOCIATION

Cu wt%	43.59	43.03	43.50	42.39	40.72	41.02	40.36	42.34 ¹⁾	39.36	41.64	40.18
Ag	0.13	d.l.	0.10	0.15	0.07	0.15	0.27	0.36	0.38	0.31	0.63
Hg	d.l.	d.l.	0.08	0.02	0.10	0.04	0.17	d.l.	d.l.	d.l.	d.l.
Zn	5.06	7.01	5.03	5.83	5.63	5.66	5.84	1.34	6.07	6.11	6.21
Cd	0.03	0.03	0.07	d.l.	d.l.	0.04	0.05	d.l.	0.07	0.07	d.l.
Fe	1.99	1.38	2.00	1.59	1.34	1.51	1.27	4.80	0.82	1.37	1.29
Co	0.03	d.l.	0.11	0.13	0.46	0.16	0.07	0.00	0.27	0.28	0.06
Ni	d.l.	d.l.	0.15	0.14	0.54	0.27	0.06	0.04	0.42	0.35	0.12
As	20.48	19.99	19.72	17.63	16.55	15.82	13.94	15.12	10.34	13.87	10.81
Sb	d.l.	0.03	0.92	1.08	0.11	0.15	0.19	4.13	7.45	9.07	10.90
Bi	d.l.	0.05	0.00	4.50	7.75	8.93	12.57	4.69	9.46	d.l.	3.72
S	28.03	27.98	28.20	27.39	26.60	26.39	25.82	26.73	25.59	27.28	26.38
Se	d.l.	d.l.	d.l.	0.05	d.l.	0.17	d.l.	0.04	d.l.	0.12	0.03
Total	99.34	99.49	99.88	100.89	99.87	100.31	100.58	99.57	100.22	100.46	100.33
Cu <i>apfu</i>	9.98	10.00	9.99	9.98	9.99	9.98	9.96	9.95	9.94	9.96	9.91
Ag	0.02		0.01	0.02	0.01	0.02	0.04	0.05	0.06	0.04	0.09
sum <i>M</i> ⁺	10.00	10.00	10.00	10.00	10.00	10.00	10.00	10.00	10.00	10.00	10.00
Cu*	0.23	0.07	0.18	0.14	0.01	0.15	0.24	0.39	0.12	0.05	0.09
Hg			0.01	0.01	0.01		0.01				
Zn	1.15	1.59	1.14	1.35	1.34	1.36	1.43	0.32	1.51	1.43	1.50
Cd			0.01			0.01	0.01		0.01	0.01	
Fe	0.53	0.37	0.53	0.43	0.37	0.42	0.36	1.33	0.24	0.37	0.36
Co	0.01		0.03	0.03	0.12	0.04	0.02		0.07	0.07	0.02
Ni			0.04	0.04	0.14	0.07	0.02	0.01	0.11	0.09	0.03
sum <i>M</i> ²⁺	1.92	2.03	1.94	1.99	1.99	2.05	2.09	2.05	2.06	2.02	2.00
As	4.07	3.97	3.91	3.57	3.45	3.31	2.99	3.13	2.24	2.83	2.28
Sb			0.11	0.13	0.01	0.02	0.02	0.53	0.99	1.14	1.42
Bi				0.33	0.58	0.67	0.97	0.35	0.74		0.28
sum <i>Y</i> ³⁺	4.07	3.97	4.02	4.03	4.04	4.00	3.98	4.01	3.97	3.96	3.98
S	13.01	12.98	13.05	12.96	12.95	12.91	12.93	12.94	12.97	12.99	13.01
Se				0.01		0.03		0.01		0.02	0.01
sum <i>Z</i> ²⁻	13.01	12.98	13.05	12.97	12.95	12.94	12.93	12.95	12.97	13.01	13.02

The number of ions is normalized to 29 atoms per formula unit (*apfu*). d.l.: detection limit. ¹⁾ ferroan tennantite. Cu* calculated as $Cu_{tot} - (10 - Ag_{tot})$.

(2002) is intergrown with berzelianite and galena and was thought to have formed at an activity of selenium (*i.e.*, $-26 < \log f(\text{Se}_2) < -31$ at 100°C), significantly lower than the peak of Se activity in the mineralizing fluid at Niederschlema-Alberoda given by the crystallization of klockmannite, which is a stable phase at $-11.6 < \log f(\text{Se}_2) < -14.3$ at the same temperature and an oxygen fugacity at the galena-anglesite buffer. Mercurian giraudite-hakite from this study occurs in a different, more complex mineral assemblage. In Figure 8, two generalized trends of the evolution of the selenium and sulfur fugacities during the deposition of the ore minerals in sample HS106 are shown. Given the presence of clausthalite (PbSe) instead of galena (PbS), the solid solutions in sample HS106 may have been deposited at Se activities higher than those supposed for mercurian giraudite-hakite in sample S55. Signs of replacement of tiemannite by mercurian giraudite (*cf.* Fig. 3a) may indicate that the reaction HgSe-Hg defines an upper limit of $f(\text{Se}_2)$ [$\log f(\text{Se}_2) = -21.4$] for the giraudite-hakite solid solutions (Fig. 8, trend 1). At a lower $f(\text{Se}_2)$, Hg did not form tiemannite but was free to

enter the structure of giraudite or hakite. Alternatively, the upper limit of $f(\text{Se}_2)$ may also be defined by the HgSe-HgS reaction, with a preferred incorporation of Hg in the tetrahedrite-tennantite and giraudite-hakite minerals instead of forming HgS (Fig. 8, trend 2). In any case, precise values for the lower limit of the activity of selenium are impossible to constrain, but are given by the PbSe-PbS univariant reaction (see Simon *et al.* 1997, their Fig. 2). Taking into account that chalcopyrite crystallized late and in equilibrium with almost Se-free tennantite, the reaction berzelianite + hematite = chalcopyrite appears to represent an appropriate upper limit of sulfur fugacity for the crystallization of giraudite and hakite. In this situation, the intersection of the reaction berzelianite + hematite = chalcopyrite with the HgSe-HgS univariant reaction would mark the upper limits of the selenium and sulfur fugacities [$\log f(\text{Se}_2) < -17.5$, $\log f(\text{S}_2) < -21$].

The paragenetic sequence implies that the tennantite-giraudite (Table 1) and tennantite-tetraedrite solid solutions (Table 3) crystallized at a similar, or slightly lower activity of selenium than the mercurian

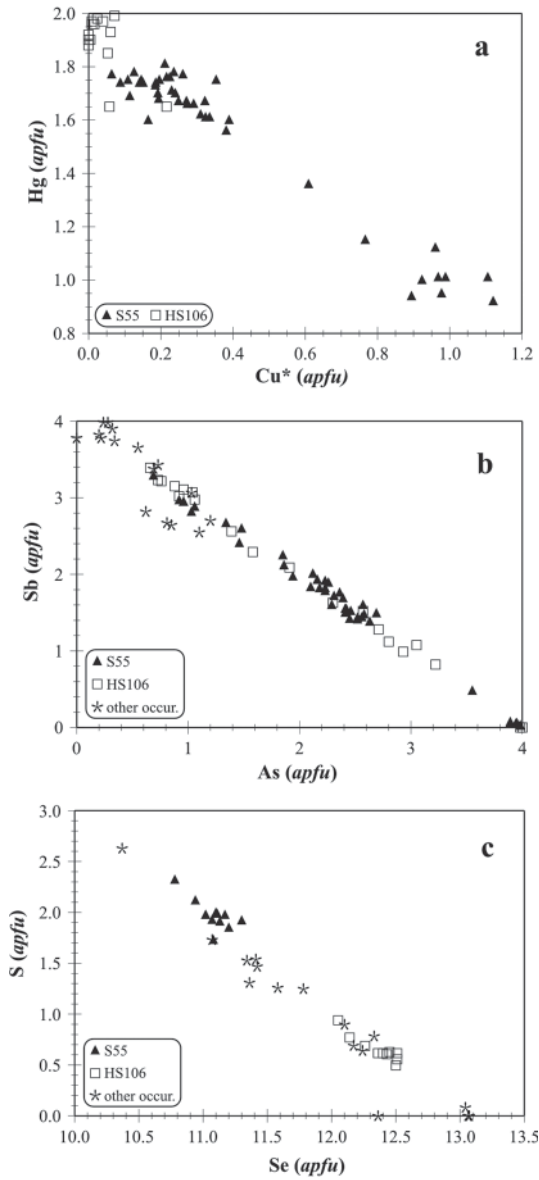


FIG. 5. Plots (in *apfu*) of Hg versus Cu* (a), Sb versus As (b), and S versus Se (c) for mercurian giraudite-hakite solid solutions in sample HS106 (this paper) and S55 (Förster *et al.* 2002) from Niederschlema-Alberoda. Note the greater extent of S-for-Se substitution and the usually higher amount of divalent copper at the M^{2+} site in the solid solutions in sample S55 relative to sample HS106. Data for other occurrences are from Johan & Kvaček (1971), Brodin *et al.* (1981), Johan *et al.* (1982), Spiridonov *et al.* (1986), Johan (1989), and Paar *et al.* (2002b).

hakite-giraudite series. However, the Se activity must have been higher than that constrained by the PbSe-PbS reaction. The Se versus S patterns of zonation are interpreted to suggest deposition from a fluid that became enriched in Se relative to S during core-to-rim crystallization of the grain shown in Figure 1. Formation of the Se-rich marginal zone caused a sudden decrease in the Se:S ratio in the fluid and deposition of Se-poor ferroan

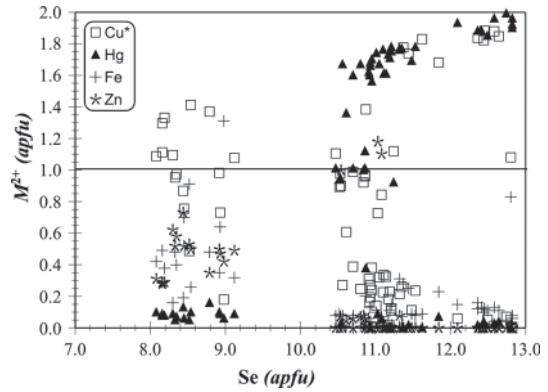


FIG. 6. Occupancy of the M^{2+} position in giraudite of various contents of Se. Data are from Johan *et al.* (1982), Förster *et al.* (2002), and this study.

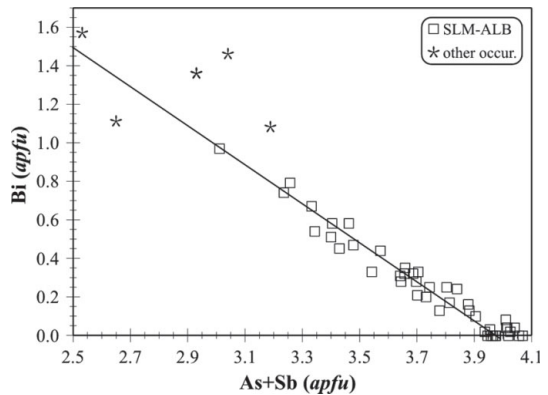


FIG. 7. Plot (in *apfu*) of Bi versus As + Sb for Bi-bearing tennantite from Niederschlema-Alberoda (SLM-ALB) and bismuthoan tennantite from other occurrences (data from Oen & Kieft 1976, Sergeyeva & Shatagin 1980, Vinogradova *et al.* 1985, Förster *et al.* 1986, Xia *et al.* 1996). Note the significant deviation from ideal stoichiometry (indicated by the full line) for most of the tennantite compositions from other occurrences. Such deviations either indicate analytical problems or, more likely, analysis of impure material.

tennantite at the lower left rim of the grain (*cf.* Figs. 2a, b). However, the Se:S ratio in the fluid underwent fluctuations and did not evolve uniformly (*cf.* Figs. 3b, c).

The Bi-bearing tennantite from the Bi–Co–Ni association (Table 4) and the tennantite from the sulfide assemblage (Table 5) formed during the Cretaceous, when the bulk of the sulfides and arsenides of Bi, Co, Ni, and Ag were deposited (*e.g.*, Schuppan *et al.* 1994, Lipp 2003). Fluid-inclusion data of Thomas & Tischendorf (1987) suggest low temperatures, similar to those during deposition of the older episode of selenide mineralization. The highest enrichment in Bi is observed in those portions of the tennantite that are closest to the relict wittichenite. These spatial relations suggest that most of the Bi that was liberated from the destabilization of Cu_3BiSe_3 immediately reprecipitated in the newly formed tennantite. This finding is consistent with the origin of other bismuthoan tennantite found as the product of replacement of associated Bi minerals (*e.g.*, Förster *et al.* 1986, and references therein). The presence of small amounts of Bi, Co, and Ni in the tennantite is a reflection of its crystallization from solutions that had earlier or simultaneously deposited the associated Bi species and Co–Ni arsenides. The temporal succession native Bi \rightarrow bismuthinite \rightarrow bismuthoan tennantite during deposition of the Bi–Co–Ni association implies

an increase in the S activity in the fluid and a crossing of the Bi– Bi_2S_3 univariant reaction at $\log f(\text{S}_2) = -22.5$ [100°C; see Simon & Essene (1996), their Fig. 12]. The assemblage chalcopyrite + pyrite + bornite + tennantite indicates that the Cretaceous tennantite (Table 5) may have formed at an activity of S exceeding that defined by the reaction chalcopyrite \rightleftharpoons pyrite + bornite at $\log f(\text{S}_2) = -16.9$ [100°C; see Simon & Essene (1996), their Fig. 13].

ACKNOWLEDGEMENTS

O. Appelt (GFZ Potsdam) is thanked for her assistance with the electron-microprobe work. G. Tischendorf (Zittau) is acknowledged for valuable comments and the performance of optical-microscope work on a selection of samples from this study. The samples were provided by G. Flach (Damme), G. Schuppan (Hartenstein), A. Hiller (Chemnitz), H. Schulz (Dresden), F. Schlegel (Schneeberg), and K. Rank (Technical University Bergakademie Freiberg). The valuable comments of W. Paar (Salzburg), an anonymous reviewer, Associate Editor F.F. Foit Jr. and Robert F. Martin helped to streamline the paper.

REFERENCES

TABLE 5. CHEMICAL COMPOSITION OF TENNANTITE FROM THE SULFIDE ASSEMBLAGE

sample anal. no.	Sh117 1	Sh117 2	Sh117 3	Sh126 4	Sh126 5	Sh126 6
Cu wt%	45.36	46.04	45.86	44.49	43.83	43.64
Ag	1.98	1.33	1.94	2.29	2.93	2.90
Hg	d.l.	0.09	d.l.	0.11	0.28	0.12
Zn	2.25	2.24	2.25	2.23	2.29	2.29
Cd	d.l.	0.04	0.06	d.l.	0.04	0.07
Fe	1.42	1.32	1.45	2.79	2.28	2.70
As	19.05	19.17	19.48	20.06	19.77	19.59
Sb	0.41	0.26	0.49	0.05	0.22	0.15
Bi	0.93	0.98	0.81	0.12	0.44	0.76
S	27.55	27.71	27.50	27.67	27.95	27.83
Se	0.06	0.05	d.l.	d.l.	d.l.	d.l.
Total	99.02	99.23	99.84	99.81	100.03	100.04
Cu <i>apfu</i>	9.72	9.81	9.73	9.68	9.59	9.60
Ag	0.28	0.19	0.27	0.32	0.41	0.40
sum M^+	10.00	10.00	10.00	10.00	10.00	10.00
Cu*	1.09	1.11	1.14	0.80	0.75	0.71
Hg		0.01		0.01	0.02	0.01
Zn	0.52	0.52	0.52	0.51	0.53	0.53
Cd			0.01		0.01	0.01
Fe	0.39	0.36	0.39	0.75	0.61	0.73
sum M^{2+}	2.00	2.00	2.06	2.07	1.92	1.99
As	3.85	3.86	3.92	4.01	3.96	3.92
Sb	0.05	0.03	0.06	0.01	0.03	0.02
Bi	0.07	0.07	0.06	0.01	0.03	0.05
sum Y^{3+}	3.99	3.96	4.04	4.03	4.02	3.99
S	13.02	13.03	12.91	12.92	13.07	13.03
Se	0.01	0.01				
sum Z^{2-}	13.03	13.04	12.91	12.92	13.07	13.03

The number of ions is normalized to 29 atoms per formula unit (*apfu*); d.l.: detection limit. Cu* is calculated as $\text{Cu}_{\text{tot}} - (10 - \text{Ag}_{\text{tot}})$. Anal. 1–5: cuprian tennantite; anal. 6: ferroan tennantite.

BRODIN, B.V., OSIPOV, B.S., KACHALOVSKAYA, V.M., KOZLOVA, YE.V. & NAZARENKO, N.G. (1981): Silver-bearing hakite. *Int. Geol. Rev.* **23**, 71–73.

FOIT, F.F., JR. & ULBRICHT, M.E. (2001): Compositional variation in mercurian tetrahedrite–tennantite from the epithermal deposits of the Steens and Pueblo Mountains, Harney County, Oregon. *Can. Mineral.* **39**, 819–830.

FÖRSTER, H.-J. (2004a): Mineralogy of the Niederschlema–Alberoda U – Se – polymetallic deposit, Erzgebirge, Germany. II. Hessite, Ag_2Te , and native Te(?), the first tellurium minerals. *Neues Jahrb. Mineral., Abh.* **180**, 101–113.

_____. (2005): Mineralogy of the Niederschlema–Alberoda U – Se – polymetallic deposit, Erzgebirge, Germany. IV. The continuous galena–clausthalite solid-solution series. *Neues Jahrb. Mineral., Abh.* (in press).

_____, COOPER, M.A., ROBERTS, A.C., STANLEY, C.J., CRIDDLE, A.J., HAWTHORNE, F.C., LAFLAMME, J.H.G. & TISCHENDORF, G. (2003): Schlemaitite, $(\text{Cu}, \square)_6(\text{Pb}, \text{Bi})\text{Se}_4$, a new mineral species from Niederschlema–Alberoda, Erzgebirge, Germany: description and crystal structure. *Can. Mineral.* **41**, 1433–1444.

_____, HUNGER, H.-J. & GRIMM, L. (1986): Elektronenstrahlmikroanalytische Untersuchungen von Erzmineralen aus der Zinn-Lagerstätte Altenberg (Erzgebirge, DDR). 4. Mitteilung: Fahlerze – Chemismus und Nomenklatur. *Chem. Erde* **47**, 111–115.

_____, RHEDE, D. & TISCHENDORF, G. (2002): Continuous solid solution between mercurian giraudite and hakite. *Can. Mineral.* **40**, 1161–1170.

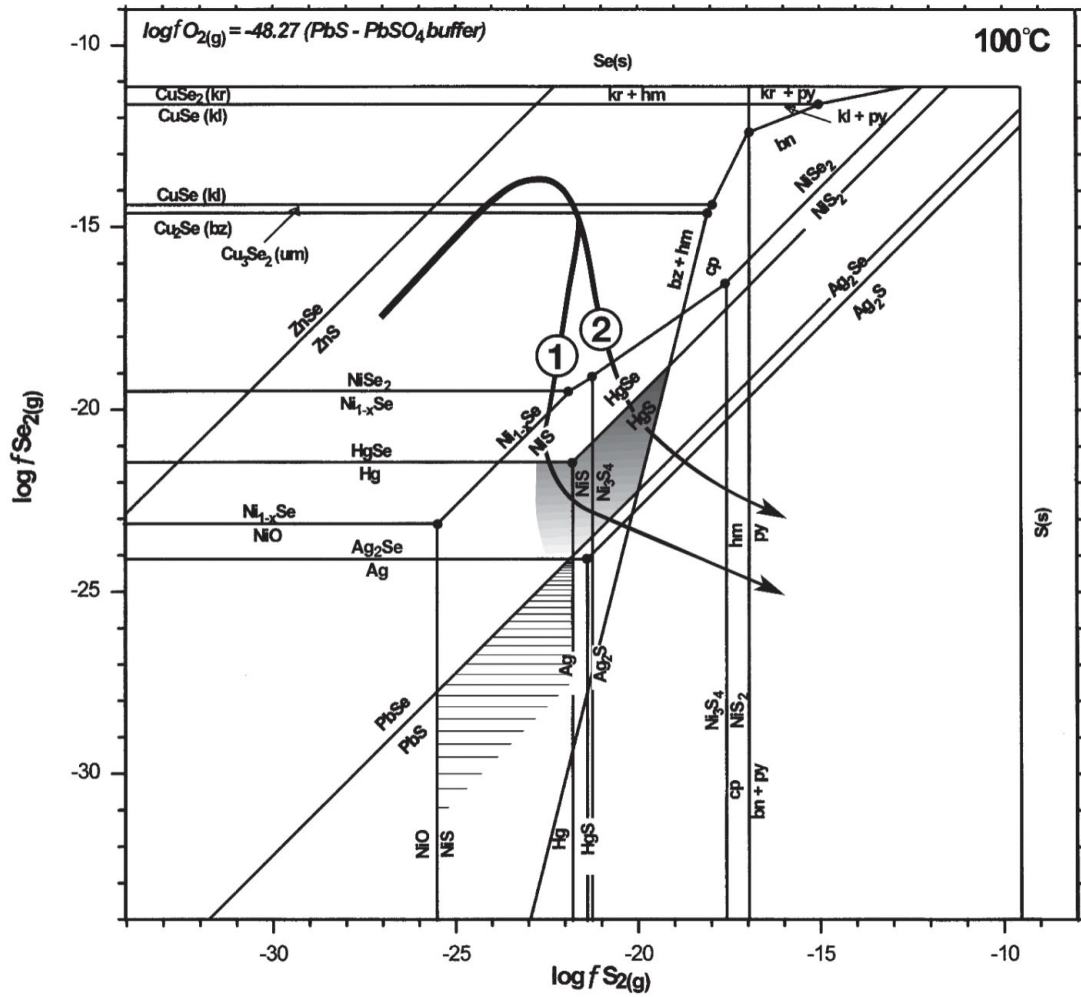


FIG. 8. Diagram showing the fugacities $f(\text{Se}_2)$ and $f(\text{S}_2)$ and the relative stabilities of some selenides and their corresponding sulfides at 100°C and at an oxygen fugacity at the anglesite–galena buffer (Simon *et al.* 1997). The arrows mark qualitatively the evolution of selenium and sulfur fugacities during the precipitation of selenides and sulfides in sample HS106, from early berzelianite to late pyrite. The fluid either may have crossed the Hg–HgSe (trend 1) or HgSe–HgS (trend 2) univariant reactions (see text for discussion). The $f(\text{Se}_2) - f(\text{S}_2)$ field for the crystallization of mercurian hakite–giraudite and giraudite–tennantite solid solutions in sample HS106 is shaded, that for mercurian giraudite–hakite solid solution in sample S55 is stippled (*e.g.*, Förster *et al.* 2002). Symbols: kr: krutaite, kd: kloekmannite, um: umangite, bz: berzelianite, hm: hematite, cp: chalcopyrite, bn: bornite, py: pyrite.

_____, _____ & _____ (2004): Mineralogy of the Niederschlema–Alberoda U – Se – polymetallic deposit, Erzgebirge, Germany. I. Jolliffeite, NiAsSe, the rare Se-analogue of gersdorffite. *Can. Mineral.* **42**, 841-849.

_____ & TISCHENDORF, G. (2001): Se-rich tennantite and constraints on P-T-X conditions of selenide mineral formation in the Schlema–Alberoda uranium ore district (western Erzgebirge, Germany). *Neues Jahrb. Mineral., Abh.* **176**, 109-126.

_____ & RHEDE, D. (2005): Mineralogy of the Niederschlema–Alberoda U – Se – polymetallic deposit, Erzgebirge, Germany. V. Watkinsonite, nevskite, bohdanowiczite and other Bi minerals. *Can. Mineral.* **43** (in press).

JOHAN, Z. (1989): Merenskyite, Pd(Te,Se)₂, and the low-temperature selenide association from the Přeborčice uranium deposit, Czechoslovakia. *Neues Jahrb. Mineral., Monatsh.* **179**-191.

- _____ & KVAČEK, M. (1971): La hakite, un nouveau minéral du groupe de la tétraédrite. *Bull. Soc. fr. Minéral. Cristallogr.* **94**, 45-48.
- _____, _____ & PICOT, P. (1978): La sabatierite, un nouveau séléniure de cuivre et de thallium. *Bull. Minéral.* **101**, 557-560.
- _____, PICOT, P. & RUHLMANN, F. (1982): Evolution paragénétique de la minéralisation uranifère de Chaméane (Puy-de-Dôme), France: chaméanite, geffroyite et giraudite, trois séléniures nouveaux de Cu, Fe, Ag et As. *Tschermaks Mineral. Petrogr. Mitt.* **29**, 151-165.
- JOHNSON, N.E., CRAIG, J.R. & RIMSTIDT, J.D. (1986): Compositional trends in tetrahedrite. *Can. Mineral.* **24**, 385-397.
- LIPP, U. (2003): Wismut-, Kobalt-, Nickel- und Silbererze im Nordteil des Schneeberger Lagerstättenbezirkes. *Bergbau in Sachsen* **10**, 209 p.
- OEN, I.S. & KIEFT, C. (1976): Bismuth-rich tennantite and tetrahedrite in the Mangualde pegmatite, Viseu district, Portugal. *Neues Jahrb. Mineral., Monatsh.*, 94-96.
- PAAR, W.H., TOPA, D., ROBERTS, A.C., CRIDDLE, A.J., AMANN, G. & SUREDA, R.J. (2002a): The new mineral species brodtkorbite, Cu_2HgSe_2 , and the associated selenide assemblage from Tuminico, Sierra de Cacho, La Rioja, Argentina. *Can. Mineral.* **40**, 225-237.
- _____, _____, _____, _____ & _____ (2002b): The new mineral species brodtkorbite, Cu_2HgSe_2 , and the associated selenide assemblage from Tuminico, Sierra de Cacho, La Rioja, Argentina: erratum. *Can. Mineral.* **40**, 989-990.
- POUCHOU, J.L. & PICOIR, F. (1985): "PAP" (ϕ - ρ - Z) procedure for improved quantitative microanalysis. In *Microbeam Analysis* (J.T. Armstrong, ed.). San Francisco Press, San Francisco, California (104-106).
- SCHUPPAN, W., BÜDER, W. & LANGE, G. (1994): On uranium mineralization in the vein deposits of the western Erzgebirge, Germany. In *Mineral Deposits of the Erzgebirge/Krušné hory* (Germany/Czech Republic) (K. von Gehlen & D.D. Klemm, eds.), Gebrüder Bornträger, Berlin, Germany (191-207).
- SERGEYEVA, N.E. & SHATAGIN, N. N. (1980): On the bismuth mineralization of the Yubileino – Shegirikhinskii deposit (Rudnyi Altai). *Dokl. Akad. Nauk SSSR* **252**, 959-962 (in Russ.).
- SIMON, G. & ESSENE, E.J. (1996): Phase relations among selenides, sulfides, tellurides, and oxides. I. Thermodynamic properties and calculated equilibria. *Econ. Geol.* **91**, 1183-1208.
- _____, KESLER, S.E. & ESSENE, E.J. (1997): Phase relations among selenides, sulfides, tellurides, and oxides. II. Applications to selenide-bearing ore deposits. *Econ. Geol.* **92**, 468-484.
- SPIRIDONOV, E.M., IGNATOV, A.I. & SHUBINA, YE.V. (1990): Evolution of fahlore composition in the Ozernoe volcanogenic deposit, Kamchatka. *Izv. Akad. Nauk SSSR, ser. geol.* **9**, 82-94 (in Russ.).
- _____, KACHALOVSKAYA, V.M. & CHVILEVA, T.N. (1986): Thallium-bearing hakite, a new fahlore variety. *Dokl. Acad. Sci. U.S.S.R., Earth Sci. Sect.* **290**, 206-208.
- _____, OKRUGIN, W.M. (1985): Selenium goldfieldite, a new fahlore variety. *Dokl. Acad. Sci. U.S.S.R., Earth Sci. Sect.* **280**, 143-145.
- THOMAS, R. & TISCHENDORF, G. (1987): Evolution of Variscan magmatic-metallogenetic processes in the Erzgebirge according to thermometric investigations. *Z. geol. Wiss.* **15**, 25-42.
- TRUDU, A.G. & KNITTEL, U. (1998): Crystallography, mineral chemistry and chemical nomenclature of goldfieldite, the tellurian member of the tetrahedrite solid-solution series. *Can. Mineral.* **36**, 1115-1137.
- VINOGRADOVA, R.A., KONONOV, O.V., BORODAYEV, YU.S., BOCHEK, L. I. & DVORTSOVA, S.P. (1985): Bismuth-bearing gray copper of the Tyrnyauz deposit. *Zap. Vses. Mineral. Obshchest.* **140**, 340-344 (in Russ.).
- XIA, XUEHUI, LIU, CHANGTAO & HUANG, FURONG (1996): The first discovery of bismuth tennantite in China. *Acta Mineral. Sinica* **16**, 274-277 (in Chinese with Engl. summary).

Received March 25, 2004, revised manuscript accepted September 14, 2004.